Research Article

Guixia Wang* and Junhong Su

Study of the length and influencing factors of air plasma ignition time

https://doi.org/10.1515/phys-2022-0067
received March 29, 2022; accepted June 06, 2022

Abstract: When a high-energy laser acts on a film surface, plasma flashes of both the air and film can be generated simultaneously. However, when the conventional plasma flash method is used to identify thin film damage, there is a misjudgment problem caused by the inability to distinguish the air and film plasma flashes. In order to solve the problem of misjudgment, the ignition times of air and thin film plasma flashes can be obtained, respectively. If the ignition times of air and thin film plasma flashes are not equal, they can be distinguished from the time difference. In this paper, a nanosecond Nd:YAG pulse laser is used to break down the air at room temperature and pressure, and the theoretical and experimental values of the ignition time of air plasma flash are obtained. The curves of the ignition time of air plasma flash with the laser wavelength, incident energy, focusing spot, and pulse width are simulated. The reasons for the changes are analyzed from the perspectives of multiphoton absorption, cascade ionization theory, and electromagnetic theory of laser breakdown gas. The results show that when the laser pulse width is 10 ns, the energy is 160 mJ, and the spot radius is 0.015 cm. The theoretical and experimental values of the ignition time of air plasma flash are 2.146 and 2 ns, respectively, which are in good agreement. Larger values of laser focus spot size and pulse width relate to a longer ignition time of the air plasma flash, whereas larger values of laser wavelength and incident energy are related to a shorter ignition time. The research reflects the characteristics and electronic transition of air plasma, as well as the micromorphological evolution of the interaction between laser and air, presents the process of air plasma flash generation and growth, and reveals the ignition mechanism of air plasma. It not only provides a basis for improving the traditional plasma flash identification method to identify film damage but also has a certain scientific significance for studying the generation mechanism of laser-supported combustion waves and detonation waves.

Keywords: laser-induced, air plasma, plasma flash, ignition time, laser parameters

1 Introduction

In a high-energy laser system, the laser-induced damage threshold (LIDT) is often used to evaluate the laser damage resistance of thin film components. The larger the LIDT of thin film, the better the laser damage resistance [1–4]. Therefore, how obtaining high LIDT has become the main bottleneck to improving the laser protection performance of thin film components. One of the keys to solving this problem is to accurately measure the LIDT of a thin film accurately. According to the test standard ISO 11254 issued by the International Committee for standardization, LIDT can be calculated by selecting the damage probability of test points within a certain range for linear fitting [5], so the accuracy of damage discrimination directly affects the accuracy of film LIDT measurement. When the traditional plasma flash method is used to judge whether the film is damaged, as long as the detector receives the film plasma flash signal, it is considered that the film has changed irreversibly and the film has been damaged. When the high-energy laser acts on the film surface, plasma flashes of both air and film can be generated simultaneously. When the detector receives the flash, it is very easy to confuse this "observable" air plasma flash with the film plasma flash, resulting in misjudgment. After the misjudgment occurs, the accuracy of the measured film LIDT will be reduced; subsequently, the determination of the anti-laser damage ability of the film is affected, which limits the development of the laser system in the direction of high power and high energy [6–9]. Obviously, in order to eliminate misjudgment, it is necessary to distinguish the difference in the time domain between the air and film plasma flashes.

* **Corresponding author: Guixia Wang,** Department of Photoelectric Engineering, Xi'an Technological University, 2 Xue Fu Zhong Lu, Wei Yang District, Xi'an, Shaanxi, 710021, China,
e-mail: noragirl6@126.com
Junhong Su: Department of Photoelectric Engineering, Xi'an Technological University, 2 Xue Fu Zhong Lu, Wei Yang District, Xi'an, Shaanxi, 710021, China

The development of air plasma is divided into four stages [10]. The first is the initial stage. In this stage, the initial electrons will be generated after the incident laser irradiates the focus, which is the initial stage of flash generation. The second is the growth stage of air plasma. In this stage, the number of free electrons and ions in the air increases rapidly due to cascade ionization, resulting in the electron density at the focus reaching the critical value ("the electron density when the air is broken down"). The third is the development stage of air plasma shock wave propagation near the focusing region, and the fourth is the disappearance stage of air plasma. The ignition time of air plasma refers to the time interval from the time when the laser is focused to the focus of the system to the time when the air produces plasma flash ignition, that is, the sum of the time required for the first and second stages.

Many scholars have done a lot of exploration around laser-induced plasma flash in the air. Mori *et al.* [11], Kim *et al.* [12], Zhou *et al.* [13], Yu-Feng *et al.* [14], and Yang *et al.* [15] studied the temporal and spatial evolution behavior of the air plasma flash phenomenon. It was found that air plasma was in the form of luminous droplets in space and expanded against the direction of the laser beam, and the air plasma flash disappeared after tens of microseconds. Jia-He *et al.* [16] of Changchun University of Technology studied the effect of gas pressure on the characteristics of nanosecond laser-induced air plasma. These studies aim to reveal the temporal and spatial evolution phenomena and laws in the process of air plasma flash and only study the duration of air plasma flash, but there are few reports on the ignition time of laser-induced air plasma flash. The literature [17,18] points out that when the laser bombards the target, the plasma flash ignition of the target is different from that of the air. Therefore, if the plasma flash ignition time of air and film can be obtained respectively, they can be accurately distinguished in the time domain to eliminate misjudgment. The purpose of this paper is to obtain the theoretical and experimental ignition time of air plasma flash (t_b) and to obtain the relationship curve of laser wavelength, incident energy, focusing spot, and pulse width affecting t_b.

2 Calculation of the ignition time of air plasma flash

2.1 Theoretical model of laser breakdown in air

Under the irradiation of a high-energy laser, there are generally two mechanisms of gas ionization: one is multiphoton absorption, and the other is cascade ionization. The first process refers to that the gas absorbs several photons at the same time, and the total energy absorbed should be equal to the ionization potential of the gas. The second process is that when the protons collide with ions, the free electrons absorb radiation until sufficient energy is obtained. Then, the atom is ionized by the inelastic collision between the electron and the atom.

In the air, there are very few free electrons in nature, and their ionization potential is very high. It is difficult for a single photon to ionize the gas. It is generally considered that air produces a small number of initial free electrons through the multiphoton absorption mechanism. These free electrons accelerate under the action of the strong electric field of the high-energy laser and ionize by collision with atoms in the air. As the numbers of free electrons increase, the collisions intensify and cascade ionization occurs. When the free electrons generated by cascade ionization exceed the loss caused by excitation, absorption, and diffusion, an air plasma area is formed. After the laser energy is absorbed by the air plasma area with a certain thickness, the temperature of the plasma area increases, the plasma expands rapidly to the surrounding air and compresses the surrounding air, the air is broken down, and the air plasma is ignited.

Because t_b is the sum of the times of initial electron generation and plasma growth stages, the first and second stages are based on multiphoton absorption and cascade ionization theory. Therefore, in order to calculate t_b, multiphoton absorption and cascade ionization theory are studied.

2.1.1 Multiphoton absorption

The multiphoton absorption process involves the simultaneous absorption of k photons by an atom having total energy not lower than the ionization potential of the atom, thus causing it to ionize. Assuming that an atom has k virtual energy states, the simultaneous absorption of k photons is equivalent to the gradual absorption of a single photon; then, the energy state increases gradually along the virtual energy level to the kth virtual energy level, which is the true energy state. In multiphoton absorption, only the states of individual atoms change; this process is independent of atom–electron collisions.

The number dn_{e1} of electrons liberated by the process of multiphoton ionization, in a volume dV during a time dt, can be written as follows

$$dn_{e1} = ANP^k dV dt. \tag{1}$$

In Eq. (1), it has been assumed that the multiphoton ionization probability for an atom can be expressed in the form AP^k, where A and k are constants for a particular gas and $P(xyzt)$ is the laser pulse profile defining its spatio-temporal characteristics, N is the density of the air molecules, and k is the number of photons that must be simultaneously absorbed to ionize an atom.

If the relative spatial distribution of the laser pulse does not change with time, then P is separable and can be written in the form $P = S(xyz)I(t)$. If we assume that the distribution $S(xyz)$ of the laser radiation is Gaussian, then we can write Eq. (1) in the following form:

$$\mathrm{d}n_{\mathrm{e1}} = \frac{ANI^k(t)\Delta V\mathrm{d}t}{k^{3/2}}. \tag{2}$$

This is the number of electrons liberated in focal volume ΔV during time dt. The k term appears in the denominator since a kth power Gaussian function has a half-width that is inversely proportional to $k^{1/2}$. The rate of change of the electron density n_{e} in the focal region due to the multiphoton ionization of the gas is thus given by [10,19]

$$\frac{\mathrm{d}n_{e1}}{\mathrm{d}t} = \frac{AN}{k^{3/2}}I^k(t), \tag{3}$$

where $I(t) = I_0 \exp\{-4\ln 2[(t-\tau_{\mathrm{p}})^2/\tau_{\mathrm{p}}{}^2]\}$ is the principle for the change of laser pulse over time, $I_0 = E/(\tau_{\mathrm{p}}\pi r^2)$ is the initial intensity of the incident laser, $A = \sigma^k/[w^{k-1}(k-1)!(\hbar w)^k]$ is the MPA rate, $w = 2\pi c/(\lambda n)$ is the optical frequency, τ_{p} is the pulse width, E is the energy of the incident laser, r is the radius of the focal point of the incident laser, σ is the photon absorption section of the atomic step, and $\hbar = 6.626 \times 10^{-34}$ is the Planck constant.

2.1.2 Cascade ionization

The area irradiated by the laser includes naturally occurring electrons and early electrons generated by multiphoton ionization, which are collectively referred to as initial electrons. Such electrons gain energy from the electric field of the laser; sufficiently large amounts of energy can cause electron–atom collision, and the atom is excited by ionization. Successive collisions develop into electron avalanches or cascade ionization. With sufficient laser energy and action time, the number of free electrons produced by the electron avalanche will exceed the losses through excitation, absorption, and diffusion. Then, the air will gradually break down and the air plasma will be ignited.

In terms of the total ionization collision frequency v, the growth of the electron density by this mechanism can be written as follows:

$$\frac{\mathrm{d}n_{\mathrm{e2}}}{\mathrm{d}t} = \nu n_{\mathrm{e}}. \tag{4}$$

This ionization collision frequency v is a linear function of the laser intensity $I(t)$; that is,

$$\frac{\nu}{N} = \left[\frac{377q}{w^2}\left(\frac{\nu_{\mathrm{m}}}{N}\right)^2\right]\cdot I(t). \tag{5}$$

The rate of change of the electron density in the cascade ionization n_{e2} with time t is shown in Eq. (6) [10,19]:

$$\frac{\mathrm{d}n_{\mathrm{e2}}}{\mathrm{d}t} = n_{\mathrm{e}}N\left[\frac{377q}{w^2}\left(\frac{\nu_{\mathrm{m}}}{N}\right)^2\right]\cdot I(t), \tag{6}$$

where q is the air coefficient, ν_{m} is the electron collision frequency for momentum transfer, $c = 3 \times 10^8$ m/s is the speed of light, λ is the wavelength of the incident laser, and $n = 1.0003$ is the refractive index of air.

By combining Eqs. (3) and (6), the electron density (n_{e}) of a specific gas over time (t) while taking multiphoton absorption and cascade ionization into account is calculated. The merged equation can be obtained as follows:

$$\frac{\mathrm{d}n_e}{\mathrm{d}t} = n_{\mathrm{e}}N\left[\frac{377q}{w^2}\left(\frac{\nu_{\mathrm{m}}}{N}\right)^2\right]\cdot I(t) + \frac{\mathrm{AN}}{k^{\frac{3}{2}}}I^k(t). \tag{7}$$

2.2 Calculation of ignition time

In Eq. (7), $N = 2.7 \times 10^{19}\,(\mathrm{cm}^{-3})$, $q = 10^{21}\,(\mathrm{cm}^{-1}\,\mathrm{s}^{-1}\,\mathrm{V}^{-2})$, $\nu_m = 3.9477 \times 10^{13}\,(\mathrm{s}^{-1})$, $\nu = 10^{15}\,(\mathrm{s}^{-1})$, $\sigma = 10^{-16}\,(\mathrm{cm}^{-2})$, $\lambda = 1.064 \times 10^{-6}\,(\mathrm{m})$, $\tau_{\mathrm{p}} = 10^{-8}\,(\mathrm{s})$, and $r = 0.015$ (cm). In the air at normal temperature and pressure, the moment of air breakdown can be defined as that at which the electron density is equal to the moment corresponding to $n_{\mathrm{e}} = 10^{13}\,\mathrm{cm}^{-3}$, which occurs when the air has broken down and the air plasma has been ignited [19]. If the laser energy is 160 mJ, the ignition time t_{b} of the air plasma flash is 2.146 ns, as shown in Figure 1.

3 Measurement of the ignition time of air plasma flash

3.1 Experimental theory

The scheme of the experiment is shown in Figure 2. The experiment uses a high-power Nd:YAG solid-state laser. The laser wavelength is 1,064 nm, the energy range is

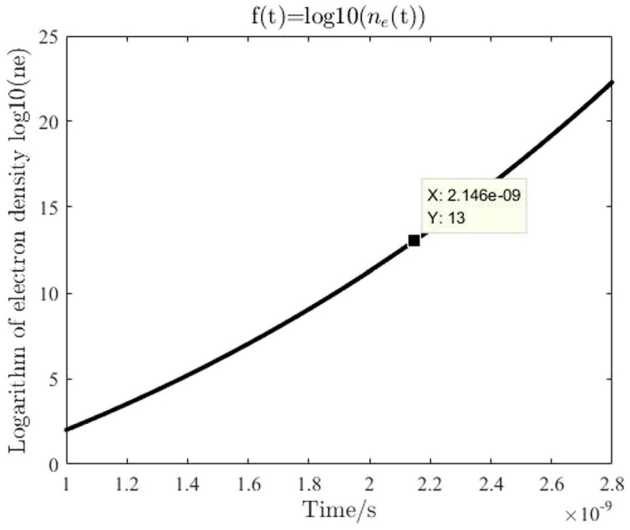

Figure 1: Calculation of air plasma flash ignition time *via* simulation.

5–235 mJ, the focus spot radius is 0.015 cm, and the pulse width is 10 ns. To ensure the stability of the output energy of the laser, the input voltage of the laser is constant in this experiment. The laser beam is sent out by the Nd:YAG laser (1) across the filter (2) and attenuator (3), and then focused by a focusing system (4) at the sample table (7), inducing the nearby air to breakdown and causing plasma flash. An energy meter (6) is for real-time reading of the reflected light energy of a beam splitter (5), and a computer (8) is for the console table operation. Detectors (9) and (10) are photodetectors DET08CL/M and DET025AL/M, respectively, which are high-speed free-space ones, produced by Thorlabs. The maximum bandwidths of detectors (9) and (10) are 5 and 2 GHz, respectively. The collectible spectral ranges are 800–1,700 and 400–1,100 nm, and the rise times are separately less than 70 and 150 ps, respectively. In the experiment, the collected incident laser signal is used as the trigger signal to collect the air flash. The starting time of the incident laser signal from scratch is taken as time 0. The starting time of the air flash signal from scratch is found. The difference between these two times is t_b. The incident laser and the air plasma flashed signals are converted to the electrical signals, which are outputted by a four-channel oscilloscope (12) of Tektronix MSO to get the signal voltage curve with time; the difference between the two signal voltage values from the none to the corresponding time is t_b. The maximum sampling frequency of the oscilloscope (12) is 1 GHz, which ensures the incident laser and air plasma flash signals are distinguished in time. In addition, in the experiment, the cables used to connect the two detectors and the oscilloscope are the same, both of which are CA2848 SMA coaxial cables purchased from Thorlabs. Because of the high energy of the incident laser, in order to protect the detector (9), an attenuator set (11) needs to be placed in front of it.

3.2 Results and analysis

Figure 3(a) shows the original signal diagrams. To obtain signal details, Figure 3(a) was proportionately enlarged (Figure 3b). In Figure 3(b), incident laser and air plasma spark signals occurred at −1.8 ns and 0.2 ns, respectively.

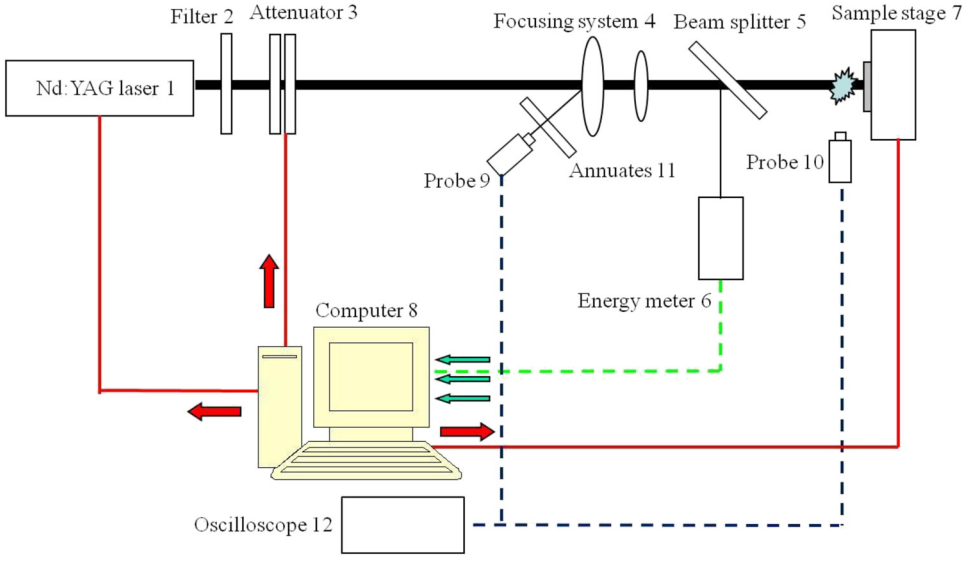

Figure 2: Schematic of the experiment.

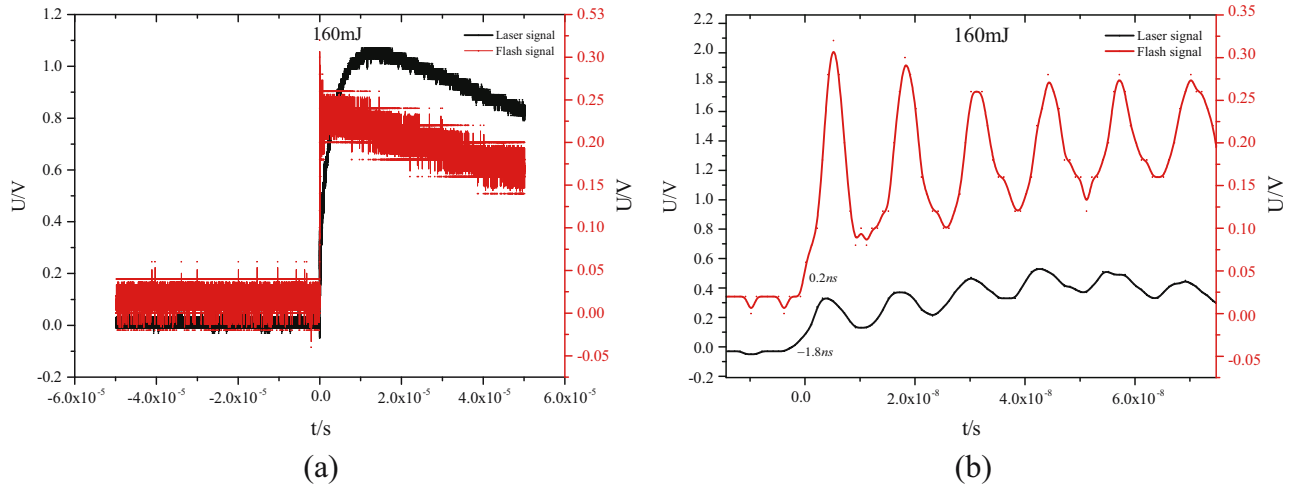

Figure 3: Signal diagram (laser intensity = 160 mJ): (a) original image, and (b) enlarged image.

Therefore, $t_b = 2$ ns. These results showed that the experimental values were similar to the theoretical values.

4 Analysis of the effect of laser parameters on the ignition time of air plasma flash

4.1 Physical process of laser breakdown of gas

The physical process of laser breakdown of gas is quite complex, and its research and understanding still needs to be further deepened. Here, a highly simplified breakdown model is proposed only from the perspective of a plasma electromagnetic field.

It can be considered that when the electric field of the laser beam is e, the force F of the laser on the free electron with charge e is determined by formula (8):

$$F = eE. \tag{8}$$

According to Newton's second law, when the electron with mass m receives the action of force F, its acceleration a is determined by Eq. (9):

$$a = \frac{F}{m} = \frac{eE}{m}. \tag{9}$$

In the time determined by the oscillation period of the oscillation field, after the free electron is accelerated, its kinetic energy is e_1, which should be:

$$e_1 = \frac{1}{2}\frac{e^2E^2}{mw^2}. \tag{10}$$

In Eq. (10), w is the angular frequency of laser radiation.

The rate at which a free electron obtains energy from an oscillating electric field dE_e/dt is

$$\frac{dE_e}{dt} = e_1\nu_0 = \frac{1}{2}\frac{e^2E^2\nu_0}{mw^2}. \tag{11}$$

In formula (11), E_e is the electron energy and ν_0 is the atomic collision frequency.

Obviously, the energy absorption rate of the laser field is directly related to t_b, and t_b decreases with an increase of dE_e/dt.

In addition, due to the complexity of air plasma ignition, it is also related to many factors, such as laser parameters, focusing parameters, air temperature, humidity, and air pressure. If it is assumed that electron diffusion and adhesion of air in the breakdown process are ignored, and the focusing parameters, air temperature, humidity, and air pressure are reasonably designed and prepared; the main influence on the ignition time of air plasma is of laser parameters. In the following, laser parameters such as laser wavelength, incident energy, focusing spot, and pulse width are changed to study their effects. Under the condition that other conditions remain unchanged, according to the theoretical model of laser breakdown of air, the variation curves of laser wavelength, laser incident energy, laser focusing spot size, and laser pulse width are simulated, respectively. The results are shown in Figures 4–7.

4.2 Laser wavelength

The t_b curves under the action of different laser wavelengths are shown in Figure 4(a). Figure 4(a) shows

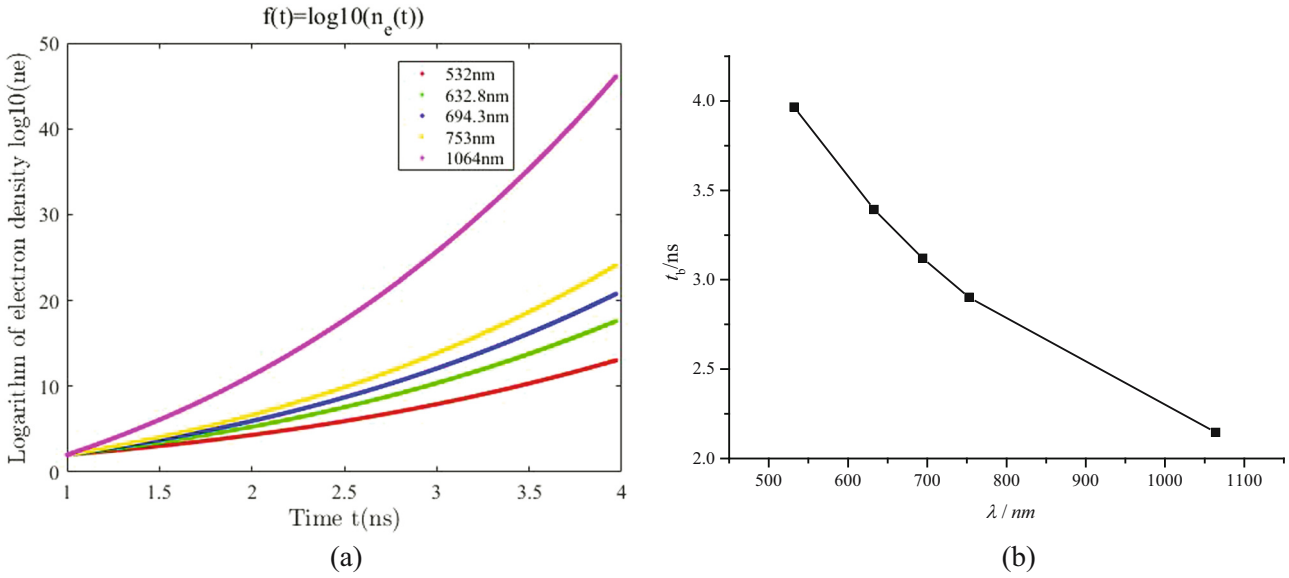

Figure 4: The t_b *vs* incident laser wavelength (r = 0.015 cm, $\tau_p = 10^{-8}$ s, E = 160 mJ): (a) the t_b curves under the action of different laser wavelengths, and (b) the variation in t_b with laser wavelength.

that under other conditions remaining unchanged, the longer the incident laser wavelength, the smaller the laser frequency, the greater the multiphoton absorption rate, the greater the degree of cascade ionization, the more intense the electron collision, and the shorter the time required to ionize the same atom. Therefore, the shorter the time to reach the electron avalanche. Therefore, a shorter electron avalanche time is related to a smaller t_b.

The variation in t_b with the incident laser wavelength is shown in Figure 4(b). In the simulation process, five wavelengths are used to calculate the corresponding t_b values. The t_b values corresponding to different wavelengths are given in Table 1. Obviously, t_b decreases with an increase in incident laser wavelength.

In addition, according to Eq. (11) in the analysis of the physical process of laser breakdown of gas, the rate at which electrons absorb energy from the laser field

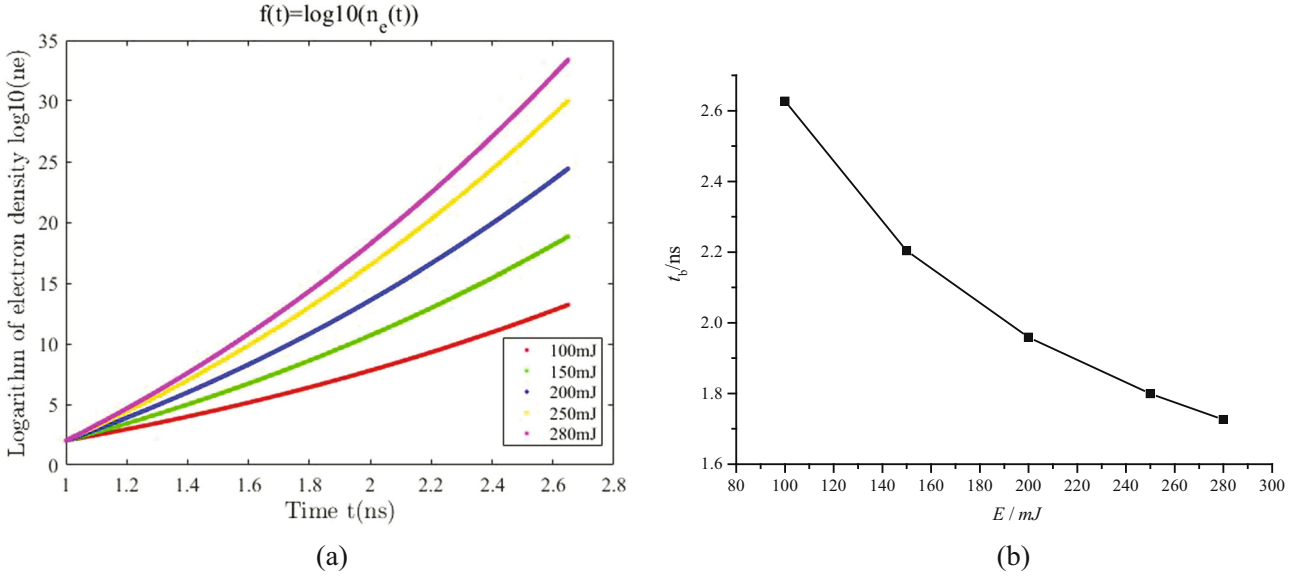

Figure 5: The t_b *versus* incident laser energy (r = 0.015 cm, $\tau_p = 10^{-8}$ s, $\lambda = 1.064 \times 10^{-6}$ m); (a) the t_b curves for different incident laser energies, and (b) the variation in t_b with incident laser energy.

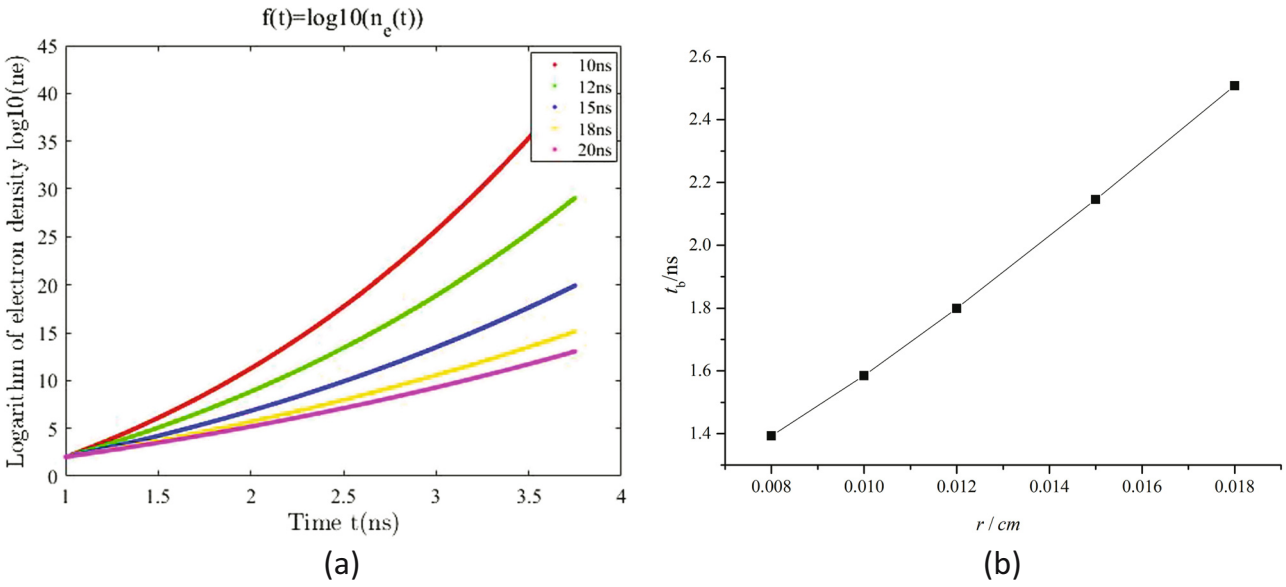

Figure 6: The t_b *versus* laser pulse width ($\lambda = 1.064 \times 10^{-6}$ m, $r = 0.015$ cm, $E = 160$ mJ): (a) the t_b curves under different laser pulse widths, and (b) the variation in t_b with laser pulse width.

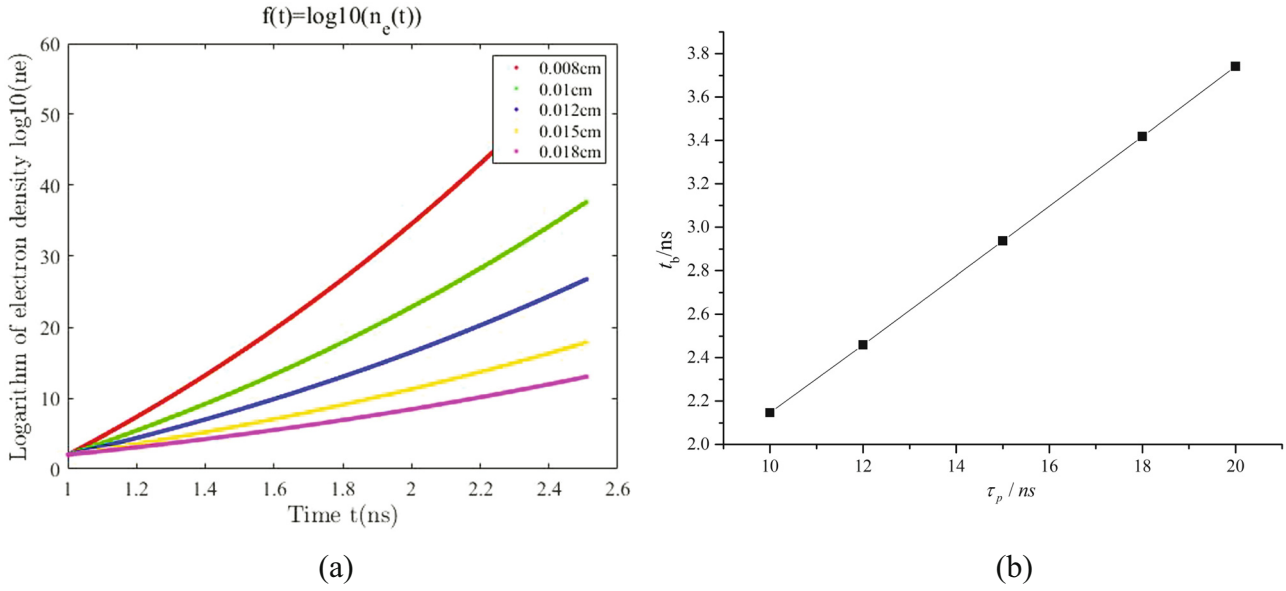

Figure 7: The t_b *vs* laser focus radiuses ($\lambda = 1.064 \times 10^{-6}$ (m), $\tau_p = 10^{-8}$(s), $E = 160$ (mJ)); (a) the t_b curves for different laser focus radiuses, and (b) the variation in t_b with laser focus radius.

increases with a decrease in the angular frequency of laser radiation, and the angular frequency of laser radiation is inversely proportional to the laser wavelength. Therefore, dE_e/dt increases with an increase in the laser wavelength, and the larger the dE_e/dt, the smaller the t_b; hence, t_b decreases with an increase in the incident laser wavelength.

Obviously, both simulation results obtained from the theoretical model of laser breakdown of air and the

Table 1: The t_b of different laser wavelengths

Laser wavelength (nm)	t_b (ns)
532	3.965
632.8	3.393
694.3	3.120
753	2.901
1,064	2.146

Table 2: The t_b of different incident laser energies

Incident laser energy (mJ)	t_b (ns)
100	2.627
150	2.204
200	1.959
250	1.799
280	1.726

analysis of the electromagnetic field of laser breakdown of gas have reached a consistent conclusion: t_b decreases with an increase in incident laser wavelength.

4.3 Laser incident energy

The t_b curves *versus* incident laser energy are shown in Figure 5(a). When all other conditions remained unchanged, from the microscopic point of view, the greater the incident laser energy, the greater the laser energy absorbed by the air, the earlier the ionization of the air, and then the earlier the generation of high-temperature and high-density plasma. This plasma absorbs the residual energy of the laser and expands rapidly to form a plasma flash faster. From a macro-level perspective, the greater the incident laser energy, the shorter the time it takes for air to ionize the same atom after absorbing energy; therefore, t_b will be smaller.

The variation in t_b with the incident laser energy is shown in Figure 5(b). In the simulation process, five kinds of laser incident energies are used to calculate the corresponding t_b values. The t_b values corresponding to different laser incident energies are given in Table 2. Obviously, t_b decreases with an increase in laser incident energy.

In addition, according to Eq. (11) in the analysis of the physical process of laser breakdown of gas, the rate of energy absorbed by electrons from the laser field increases with an increase in laser beam electric field E, and the laser beam electric field E is directly proportional to the laser incident energy. Therefore, dE_e/dt increases with an increase in laser incident energy, and the larger the dE_e/dt, the smaller t_b, so t_b decreases with an increase in laser incident energy.

Obviously, both the simulation results obtained from the theoretical model of laser breakdown of air and the analysis of the electromagnetic field of laser breakdown of gas have reached a consistent conclusion: t_b decreases with an increase in incident laser energy.

4.4 Laser pulse width

The t_b curves *versus* laser pulse width are shown in Figure 6(a). When all other conditions remained unchanged, a smaller laser pulse width was related to a higher incident laser power, and less time was required for the incident laser power density to reach the air plasma ignition threshold, thus resulting in quicker plasma flashes and smaller t_b.

The variation in t_b with the laser pulse width is shown in Figure 6(b). In the simulation process, five laser pulse widths are used to calculate the corresponding t_b values. The t_b values corresponding to different laser pulse widths are shown in Table 3. Obviously, t_b increases with an increase in laser pulse width.

Canavan *et al.* [20] reported that the threshold intensity of air breakdown (unit: W/cm^2) changes with the change of laser pulse width. When the laser pulse width is less than 10^{-7} s, the threshold intensity of air breakdown decreases with an increase in laser pulse width at 1 atm. According to the ignition mechanism of air plasma, the smaller the threshold intensity of air breakdown, the slower the ignition of air plasma; so, t_b is larger, which is consistent with the results analyzed in this paper.

4.5 Laser focus radius

The t_b curves *versus* laser focus radii are shown in Figure 7(a). When all other conditions remained unchanged, a smaller

Table 3: The t_b of different laser pulse widths

laser pulse width (ns)	t_b (ns)
10	2.146
12	2.459
15	2.937
18	3.419
20	3.742

Table 4: The t_b of different laser focus radii

Laser focus radius (cm)	t_b (ns)
0.008	1.393
0.01	1.585
0.012	1.799
0.015	2.146
0.018	2.508

laser focus radius was related to higher energy per unit area in the focus region and a smaller laser focus radius.

The variation in t_b with laser focus radius is shown in Figure 7(b). In the simulation process, five laser focusing spots are used to calculate the corresponding t_b values. The t_b values corresponding to different laser focusing spots are shown in Table 4. Obviously, t_b increases with an increase in laser focusing spots.

Brown [21] reported that the threshold intensity of air breakdown (unit: W/cm^2) changes with the change of laser focusing radius. When the laser focusing radius changes from 10^{-2} to 10^{-1} cm, the threshold intensity of air breakdown decreases. According to the ignition mechanism of air plasma, the smaller the threshold intensity of air breakdown, the slower the air plasma ignition; so, t_b is larger, that is, t_b increases with an increase in laser focus spot. This is also consistent with the results of this paper.

In summary, the analysis revealed that when all the other conditions remain unchanged, a larger laser focus spot size and pulse width are related to a larger t_b value, whereas a longer laser wavelength and larger incident energy are related to a smaller t_b value.

5 Conclusions

DC electric field, RF, microwave source and laser can be used as radiation sources for gas breakdown. The mechanism of gas breakdown of each radiation source is different. In this paper, laser breakdown of gas is used. There are many applications for laser breakdown of gas to produce high-temperature and high-density plasma, such as laser-generated controllable fusion, laser radiation heating plasma and so on. In the research field of laser radiation interaction, the discussion of a plasma source with high intensity, high density, and high temperature will have wide application value. In this paper, the theoretical and experimental values of the ignition time of air plasma flash are obtained, and and the relationship between ignition times and laser parameters is simulated. The reasons for the change are analyzed from the perspectives of multiphoton absorption, cascade ionization theory, and electromagnetic theory of laser breakdown of gas. It reflects the characteristics and electronic transition of air plasma, as well as the micromorphological evolution of the interaction between laser and air, presents the process of air plasma flash generation and growth, reveals the ignition mechanism of air plasma, eliminates the misjudgment of the plasma flash method, and provides an idea for the study of laser radiation interaction from the perspective of ignition time.

On the applicability of the results of this paper, the following can be concluded:

1) Because the multiphoton absorption process is particularly sensitive to the energy difference between the photon energy and the ionization potential of the gas; that is, the greater the energy difference, the greater the photon energy that needs to be absorbed at the same time in order to realize gas ionization, and the smaller the probability. Therefore, the multiphoton absorption process can be observed only when the photon energy is about 1 eV or more; that is, the multiphoton absorption process can be observed when the laser wavelength is less than 1.1 μm. In this paper, the laser photon energy emitted by the nanosecond Nd:YAG 1,064 nm pulse laser is about 1.2 eV, and the multiphoton absorption process can be observed. Therefore, the theoretical model for calculating t_b in this paper is suitable for lasers with wavelengths shorter than 1.1 μm.
2) All experimental results given in this paper are based on the existing laser film damage testing instruments in the laboratory. The experimental data and conclusions obtained have some limitations, but they can also provide a reference for the experimental study of air plasma flash.
3) The ignition process of laser breakdown of air plasma is very complex. In this paper, only the effects of laser wavelength, incident energy, focusing spot, and pulse width on t_b are analyzed. In fact, it is also related to the gas type and pressure, temperature, humidity, preionization, and other parameters, which may be a direction of our follow-up research.

Funding information: This work was supported in part by the National Natural Science Foundation of China (NSFC) (No. 61378050).

Author contributions: All authors have accepted responsibility for the entire content of this manuscript and approved its submission.

Conflict of interest: The authors state no conflict of interest.

References

[1] Lai QY, Feng GY, Yan J, Han J, Zhang L, Ding K. Damage threshold of substrates for nanoparticles removal using a laser-induced plasma shockwave. Appl Surf Sci. 2021;539:148282.

[2] Zhu CQ, Dyomin V, Yudin N, Antipov O, Verozubova G, Eranov I, et al. Laser induced damage threshold of nonlinear GaSe and GaSe:In crystals upon exposure to pulsed radiation at a Wavelength of 2.1 μm. Appl Sciences-Basel. 2021;11(3):1208.
[3] Xie LY, Zhang JL, Zhang ZY, Ma B, Li T, Wang Z, et al. Rectangular multilayer dielectric gratings with broadband high diffraction efficiency and enhanced laser damage resistance. OPT Express. 2021;29(2):2669–78.
[4] Lian X, Yao WD, Liu WL, Tang RL, Guo SP. KNa2ZrF7: A mixed-metal fluoride exhibits phase matchable second-harmonic-generation effectand high laser induced damage threshold. Inorg Chem. 2021;60(1):19–23.
[5] Shan C, Zhao YA, Zhang XH, Hu GH, Wang YL, Peng XC, et al. Study on laser damage threshold of optical element surface based on gaussian pulsed laser spatial resolution. Chin J Lasers. 2018;45(1):0104002.
[6] Ling XL, Liu SH, Liu XF. Enhancement of laser-induced damage threshold of optical coatings by ion-beam etching in vacuum environment. Optik. 2020;200:163429.
[7] Kumar S, Shankar A, Kishore N, Mukherjee C, Kamparath R, Thakur S. Laser-induced damage threshold study on TiO_2/SiO_2 multilayer reflective coatings. Indian J Phys. 2020;94:105–15.
[8] Li YY, Zhang WY, Liu Z, Li MX, Fu XH. Cumulative effect of thin film laser damage under S-on-1 measurement mode. Laser Technol. 2018;42(1):39–42.
[9] Xu C, Yi P, Fan HL, Qi JW, Yang S, Qiang YH, et al. Preparation of high laser-induced damage threshold $Ta2O_5$ films. Appl Surf Sci. 2014;309:194–9.
[10] Morganz CG. Laser-induced breakdown of gases. Rep Prog Phys. 1975;38:623.
[11] Mori K, Komurasaki K, Katsurayama H. Laser produced plasma in high-speed flows. 24th International Congress on High-speed Photography and Photonics. Vol. 4183, SPIE; 2001. p. 829–36.
[12] Kim JU, Lee HJ, Kim C. Characteristics of laser-produced plasmas in a gas filled chamber and in a gas jet by using a long pulse laser. J Appl Phys. 2003;94(9):5497–503.
[13] Zhou J, Feng LW, Liu Y, Xu ZH. Laser-induced plasma by high speed photography. J Appl Opt. 2011;32(5):1027–31.
[14] Liu YF, Ding YJ, Peng ZM, Hang Y, Du YJ. Spectroscopic study on the time evolution behaviors of the laser-induced breakdown air plasma. Acta Phys Sin. 2014;63(20):205205.
[15] Yang ZF, Wei WF, Han JX, Wu J, Li XW, Jia SL. Experimental study of the behavior of two laser produced plasmas in air. Phys Plasmas. 2015;22(7):073511.
[16] Liu JH, Lu JZ, Lei JJ, Gao X, Lin JQ. Effect of ambient gas pressure on characteristics of air plasma induced by nanosecond laser. Acta Phys Sin. 2020;69(5):057401.
[17] Chen L, Lu JY, Wu, JY, Feng, CG. Laser supported detonation wave. Beijing: National Defence Industry Press; 2011. p. 27.
[18] Wang GX, Su JH, Xu JQ, Yang LH, Wu SJ. Research on the ignition time of laser-induced film plasma and its influence factors. Acta Optica Sin. 2017;37(4):0431001.
[19] Lu J, Ni XW, He AZ. Physics of interaction between laser and materials. Beijing: China Machine Press; 1996. p. 10.
[20] Canavan GH, Proctor W, Nielsen PE, Rockwood SD. CO_2 laser air breakdown calculations. IEEE JQuantum Electron. 1972;8(6):564–5.
[21] Brown SC. Microwave gas discharge breakdown. Appl Sci Res Sect B. 1956;5(1):97–108.